J|A|C|S COMMUNICATIONS

Published on Web 09/01/2009

Hydrogen-Bonding-Assisted Self-Assembly: Monodisperse Hollow Nanoparticles Made Easy

Zaicheng Sun,[†] Feng Bai,[†] Huimeng Wu,[‡] Samantha K. Schmitt,[†] Daniel M. Boye,[§] and Hongyou Fan*[,‡,†]

NSF Center for Micro-Engineered Materials, Chemical and Nuclear Engineering Department, The University of New Mexico, Albuquerque, New Mexico 87131, Advanced Materials Lab, Sandia National Laboratories, Albuquerque, New Mexico 87106, and Physics Department, Davidson College, Davidson, North Carolina 28035

Received July 6, 2009; E-mail: hfan@sandia.gov

Because hollow nanoparticles play important roles in many applications, including catalysis and nanoreactors, optics, sensing, and controlled release, there have been numerous synthesis efforts.[1−6] Hollow particles or nanostructures have been synthesized primarily through the "template method". Through the use of colloid particles with reactive surfaces as templates, both inorganic and polymer hollow particles have been prepared.[1,2,5,7−9] Block copolymer self-assembly has been developed to form hollow vesicles or capsules and hybrid organic−inorganic hollow nanoparticles.[10−14] A freeze-dry process was developed to prepare hollow polymer particles.[15] Recently, through a spontaneous dissolution−regrowth process, uniform hollow silica colloids were synthesized with an average particle size of 300 nm.[16] The development of more facile and efficient methods for synthesis of monodisperse hollow nanoparticles is critically important for the continued advancement of this area. Here we report a new facile self-assembly technique for synthesizing monodisperse hollow spherical nanoparticles that are less than 50 nm in diameter. Preferential hydrogen bonding between an amphiphilic block copolymer and a hydrogen-bonding agent (HA) enables formation of monodisperse spherical solid polymer nanoparticles with the HA residing in the particle core surrounded by the polymer. Removal of the HA results in monodisperse hollow nanoparticles with tunable hollow cavity size and surface reactivity.

Scheme 1. (i) Hydrogen-Bonding-Assisted Self-Assembly and (ii) Formation of Hollow Nanoparticles

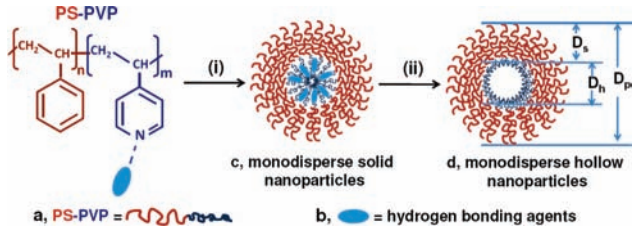

Scheme 1 describes the hydrogen-bonding-assisted self-assembly process and the formation of hollow nanoparticles. The amphiphilic block copolymer was polystyrene-*b*-polyvinylpyridine (PS-PVP). 2-(4′-Hydroxybenzeneazo)benzoic acid (HBBA) was used as the HA. For a typical synthesis, we added a 2 wt % solution of HBBA in dioxane to a 2−4 wt % solution of PS-PVP in dioxane. After the mixture was stirred and heated (70 °C) for up to 10 h, the nanoparticles were collected through centrifugation. Formation of hydrogen bonds between the −COOH groups of HBBA and the hydrophilic PVP chains[17] facilitates phase separation, producing solid nanoparticles with HBBA in the particle core (process i). This was confirmed by dynamic light scattering results (Figure S1 in the Supporting Information). Before addition of HBBA, PS-PVP disperses in solvents without phase separation. Addition of HBBA induces PS-PVP phase separation and nanoparticle formation in the solution. Removal of HBBA was conducted using an alcohol (methanol or ethanol) wash. Alcohols are good solvents for PVP chains and nonsolvents for PS chains. During the alcohol wash, the preferential solvation of the PVP chains with alcohol breaks the hydrogen bonds between the PVP chains and HBBA; the alcohol then dissolves and selectively removes the HBBA to form hollow nanoparticles (process ii). The scanning electron microscopy (SEM) image in Figure 1A shows as-prepared polymer nanoparticles obtained using 2 wt % PS-PVP and 2 wt % HBBA before removal of HBBA. The nanoparticles were monodisperse with an average diameter (D_p) of 35 nm and a narrow size distribution [standard deviation (σ) of <7%]. The Figure 1A inset shows a transmission electron microscopy (TEM) image of these nanoparticles. The uniform electron contrast across each nanoparticle suggests that the nanoparticles are solid particles. The TEM image recorded after removal of HBBA by the alcohol wash (Figure 1B) shows evident electron contrast between the cores and shells of the particles, confirming the formation of hollow particles. The TEM image also reveals that the hollow nanoparticles remain spherical in shape after removal of HBBA, demonstrating their stability. The formation of hollow nanoparticles further confirms that HBBA associates with PVP chains and resides at the nanoparticle core surrounded by PS. Because of the monodispersity, the hollow nanoparticles form large areas of ordered arrays (Figure 1B and Figure S6). By careful control of the molar ratio of HBBA to PVP, we determined a HBBA/PVP molar ratio threshold of ∼1.5 above which the hollow diameter (D_h) does not increase. Any extra HBBA crystallizes in solution. Below the threshold, we can control D_h from several nanometers up to tens of nanometers by gradually increasing the chain length of polymer and/or amount of HBBA (see Figures S2 and S3).

The hollow nature and the accessibility of the cavity were further verified by nitrogen sorption measurements using a surface acoustic wave technique.[18] Figure 1C compares nitrogen sorption isotherms of solid and hollow nanoparticle films at 77 K. Both films followed type-IV sorption isotherms. The solid nanoparticle films showed a dramatic nitrogen uptake starting at $P/P_0 \approx 0.8$ with a small hysteresis, suggesting the existence of large mesopores.[19] This is due to the gaps between neighboring nanoparticles. After removal of HBBA, the hollow nanoparticle film exhibited an H1-type hysteresis loop, with almost vertical steps on the ascending and descending curves starting at $P/P_0 \sim 0.8$, which is characteristic of a mesoporous material with a narrow pore size distribution. The

[†] The University of New Mexico.
[‡] Sandia National Laboratories.
[§] Davidson College.

10.1021/ja905240w CCC: $40.75

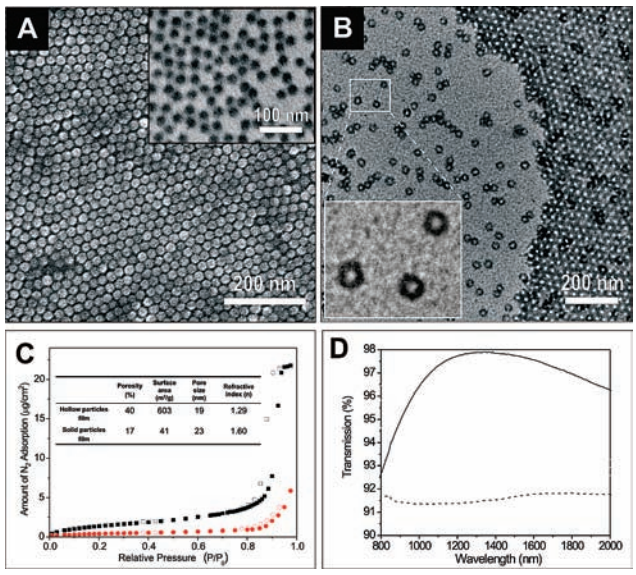

Figure 1. (A) Representative SEM image of monodisperse solid polymer nanoparticles prepared using 2 wt % $PS_{19.9k}$-$PVP_{29.4k}$ and 2 wt % HBBA. Because of the monodispersity, the nanoparticles form ordered hexagonal arrays. Inset: TEM image revealing that the nanoparticles are solid. (B) Representative TEM image of the specimen in (A) after removal of HBBA by the alcohol wash. The large-area ordered arrays of hollow nanoparticles on the right part of the image consist of individual hollow nanoparticles like those shown in the left part of the image. The inset square box highlights three individual hollow nanoparticles. Figure S6 shows three-dimensionally ordered arrays of solid and hollow nanoparticles. (C) Nitrogen sorption isotherms obtained at 77 K for (circles) a solid nanoparticle film prepared with 2 wt % PS_{20k}-PVP_{19k} and 2 wt % HBBA and (squares) a hollow nanoparticle film after removal of HBBA (adsorption, solid data markers; desorption, open data markers). The films were applied to an area of ~1 cm^2 on a piezoelectric ST-cut quartz substrate with interdigital gold transducers designed to operate at ~97 MHz. Mass change was monitored (~80 pg cm^{-2} sensitivity) as a function of relative pressure using a surface acoustic wave technique. The inset table shows the porosities, surface areas, pore sizes, and refractive indexes of the two nanoparticle films. (D) Light transmission vs wavelength for microscope glass slides that were covered on both sides with a 256 nm thick film of hollow nanoparticles serving as an AR coating. The nanoparticle coating prepared using hollow nanoparticles (solid line) exhibited a light transmission of ~98% at ~1250 nm. Results for an uncoated glass slide (dashed line) are shown for comparison.

measured surface areas of both the solid and hollow nanoparticle films demonstrate the accessibility of the hollow cavities and the mesoporosity between neighboring nanoparticles. Subtraction of the porosity of the solid particle film from that of the hollow-particle film gives a porosity of 23% resulting from the hollow cavities. Visible ellipsometric data for this film before and after removal of HBBA were fitted with refractive indices (n) of 1.63 and 1.30, respectively, at 550 nm. The decrease in n is due to the presence of the hollow cavity. By controlling the amount of added HBBA, we tuned the index of refraction from that of the solid PS-PVP (1.64) down to 1.20 at 550 nm. With such a low n and pore and particle sizes less than 50 nm, the hollow nanoparticle films are viable alternatives for antireflective (AR) coatings. Figure 1D compares the transmission of a bare-glass slide and a hollow-nanoparticle-coated glass slide. The hollow-nanoparticle-coated glass slide showed ~98% transmission in the near-IR spectrum, which is better than the optimium value of the inorganic coating material MgF_2 (~97.5%).

Removal of HBBA results in empty space and available nitrogen (−N═) from PVP chains on the inner surface, providing a well-defined nanocavity and surface reactive sites for further introduction of functional elements. To demonstrate the reactivity of the inner surface of the hollow cavity, we prepared hybrid nanoparticles containing TiO_2 nanoparticles by introduction of titanium(IV) *tert*-butoxide (TBO) (Figure S4). Hydrolysis and condensation of TBO produced hydroxylated oligomers or nanoclusters associated with PVP through hydrogen bonding between the hydroxyl groups and nitrogen (−N═) of the PVP chains. Further nucleation and growth of TiO_2 nanoparticles were thus confined within the hollow cavities. Besides TiO_2, we extended the method to the synthesis of hybrid nanoparticles containing silica or tungsten oxide nanoparticles (Figure S5).

In summary, our method is a facile process for synthesizing monodisperse hollow nanoparticles with controlled hollow cavity size and internal surface reactivity. Formation of large areas of uniform films of ordered hollow nanoparticle arrays allows practical utilization of these nanoparticles in applications such as membrane separation[20] and catalysis and sensing[3] and as nanoreactors[3] for the synthesis of complex organic, inorganic, and biospecies assemblies in general. The robustness of our method enables the fabrication of hybrid polymer−inorganic nanoparticles.

Acknowledgment. This work was supported by the U.S. Department of Energy (DOE) Basic Energy Sciences (BES) Program, Sandia National Laboratory's Laboratory Directed Research and Development (LDRD) Program, the National Science Foundation (DMI-0625897), and CRADA. TEM studies were performed at the Department of Earth and Planetary Sciences at the University of New Mexico. We acknowledge the use of the SEM facility supported by the NSF EPSCOR and NNIN grants. Sandia is a multiprogram laboratory operated by Sandia Corporation, a Lockheed Martin Company, for the U.S. DOE's National Nuclear Security Administration under Contract DE-AC04-94AL85000.

Supporting Information Available: Full experimental details and characterizations. This material is available free of charge via the Internet at http://pubs.acs.org.

References

(1) Xu, X.; Asher, S. A. *J. Am. Chem. Soc.* **2004**, *126*, 7940.
(2) Caruso, F.; Caruso, R. A.; Mohwald, H. *Science* **1998**, *282*, 1111.
(3) Vriezema, D. M.; Aragones, M. C.; Elemans, J. A. A. W.; Cornelissen, J. J. L. M.; Rowan, A. E.; Nolte, R. J. M. *Chem. Rev.* **2005**, *105*, 1445.
(4) Langer, R. *Nature* **1998**, *392* (suppl.), 5.
(5) Caruso, F. *Chem.—Eur. J.* **2000**, *6*, 413.
(6) Allen, C.; Maysinger, D.; Eisenberg, A. *Colloids Surf., B* **1999**, *16*, 3.
(7) Yang, M.; Ma, J.; Zhang, C. L.; Yang, Z. Z.; Lu, Y. F. *Angew. Chem., Int. Ed.* **2005**, *44*, 6727.
(8) Yang, Z. Z.; Niu, Z. W.; Lu, Y. F.; Hu, Z. B.; Han, C. C. *Angew. Chem., Int. Ed.* **2003**, *42*, 1943.
(9) Shchukin, D. G.; Sukhorukov, G. B.; Mohwald, H. *Angew. Chem., Int. Ed.* **2003**, *42*, 4472.
(10) Discher, D. E.; Eisenberg, A. *Science* **2002**, *297*, 967.
(11) Zhang, L.; Eisenberg, A. *Science* **1995**, *268*, 1728.
(12) Dou, H. J.; Jiang, M.; Peng, H. S.; Chen, D. Y.; Hong, Y. *Angew. Chem., Int. Ed.* **2003**, *42*, 1516.
(13) Du, J. Z.; Chen, Y. M. *Angew. Chem., Int. Ed.* **2004**, *43*, 5084.
(14) Liu, X. K.; Jiang, M. *Angew. Chem., Int. Ed.* **2006**, *45*, 3846.
(15) Im, S. H.; Unyong, U.; Xia, Y. *Nat. Mater.* **2005**, *4*, 671.
(16) Zhang, T. R.; Ge, J. P.; Hu, Y. X.; Zhang, Q.; Aloni, S.; Yin, Y. D. *Angew. Chem., Int. Ed.* **2008**, *47*, 5806.
(17) (a) Sidorenko, A.; Tokarev, I.; Minko, S.; Stamm, M. *J. Am. Chem. Soc.* **2003**, *125*, 12211. (b) Rodriguez, A. T.; Li, X.; Wang, J.; Steen, W. A.; Fan, H. *Adv. Funct. Mater.* **2007**, *17*, 2710. (c) Rodriguez, A. T.; Chen, M.; Chen, Z.; Brinker, C. J.; Fan, H. *J. Am. Chem. Soc.* **2006**, *128*, 9276. (d) Sun, Z.; Bai, F.; Wu, H.; Schmitt, S. K.; Boye, D. M.; Jiang, Z.; Wang, J.; Fan, H. *Chem.—Eur. J.* **2009**, in press.
(18) Frye, G. C.; Ricco, A. J.; Martin, S. J.; Brinker, C. J. *Mater. Res. Soc. Symp. Proc.* **1988**, *121*, 349.
(19) Zhao, D.; Feng, J.; Huo, Q.; Melosh, N.; Fredrickson, G. H.; Chmelka, B. F.; Stucky, G. D. *Science* **1998**, *279*, 548.
(20) Bergbreiter, D. E. *Angew. Chem., Int. Ed.* **1999**, *38*, 2870.

JA905240W